DOI: 10.1021/ma101526k

Macromolecules
COMMUNICATION TO THE EDITOR

Dopamine-Induced Reduction and Functionalization of Graphene Oxide Nanosheets

Li Qun Xu,[†] Wen Jing Yang,[†] Koon-Gee Neoh,[†] En-Tang Kang,*[,†] and Guo Dong Fu*[,‡]

[†]*Department of Chemical & Biomolecular Engineering, National University of Singapore, Kent Ridge, Singapore 119260, and* [‡]*School of Chemistry and Chemical Engineering, Southeast University, Jiangning District, Nanjing, Jiangsu Province, P. R. China 211189*

Received July 8, 2010
Revised Manuscript Received September 23, 2010

Introduction. Graphene, which consists of atom-thick sheets of carbon organized in a honeycomb structure, has attracted a great deal of attention in recent years because of its unique electrical, optical, catalytic, and mechanical properties.[1−5] Many methods, such as mechanical exfoliation,[6] chemical vapor deposition (CVD),[7] and reduction of graphene oxide (GO),[8−22] have been reported for the preparation of high-quality graphene. Nevertheless, it is desirable to explore other low-cost and environmentally friendly methods for the reduction of GO in bulk quantities. The reagents commonly used for the reduction of GO are hydrazine, dimethylhydrazine, hydroquinone, and $NaBH_4$, which are either toxic or hazardous. Furthermore, the reduced GO has a tendency to agglomerate irreversibly, or even to restack into graphite through van der Waals interactions, in the absence a polymer dispersant or surfactant.[23−25] Accordingly, effective and mild means for the reduction of GO, as well as for the modification of reduced graphene oxide (RGO), to improve their stability and dispersity (and thus processability) are desirable.

The adhesive proteins of mussels, which contain high concentrations of catechol and amine functional groups, exhibit excellent affinity for most organic and inorganic surfaces, such as metal, metal oxide, and polymer surfaces.[26] Dopamine, commonly known as a hormone and neurotransmitter, is a unique molecule mimicking the adhesive proteins. At a weak alkaline pH, dopamine will undergo self-polymerization to produce an adherent polydopamine (PDA) coating on a wide range of substrates, with the accompanied oxidation of catechol groups to the quinone form.[27−29] The oxidized quinone form of catechol can undergo reactions with various functional groups, including thiol, amine, and quinone itself, via Michael addition[30] or Schiff base reaction[31] to form covalently grafted functional layers.[27,32−34] Moreover, as a good reducing agent, dopamine has recently been used to prepare polymer nanocomposites via direct redox reaction with $HAuCl_4$ and H_2PtCl_6 (the oxidants).[35,36] The fascinating (reduction, self-polymerization, and adhesion) properties of dopamine allow one to use it simultaneous as a reducing agent for GO and as a capping agent to stabilize and decorate the resulting reduced GO (RGO) surface for further functionalization. For example, the Michael addition (or Michael addition/Schiff base reaction) between the PDA-capped RGO and thiol-terminated (or amino-terminated) poly(ethylene glycol) (PEG) can give rise to functionalized RGO (Scheme 1).

Results and Discussion. The GO nanosheets were produced from natural graphite flakes by the modified Hummer's method.[37,38] PDA-capped RGO was prepared via the simultaneous reduction of GO by dopamine hydrochloride and self-polymerization of the latter (Experimental Section). The morphology of GO and PDA-capped RGO nanosheets is revealed by transmission electron microscope (TEM) images of parts a and b of Figure 1, respectively. Since PDA has a tendency to form free PDA particles at high dopamine concentration or temperature,[35] the PDA-capped RGO was filtered, washed, and dialyzed against distilled water. Arising from these treatments and high affinity of the PDA aromatic rings for graphene, no free PDA particles were observed in the TEM images of PDA-capped RGO nanosheets. The reduction process of GO by dopamine in Tris-Cl was monitored by UV−vis absorption spectroscopy. In Figure 2, the absorbance peaks at 230 and 300 nm, characteristic of GO, have shifted to 268 nm, and the intensity of the absorption tail in the visible region (> 300 nm) has increased with the reduction time while the PDA-capped RGO remains uniformly dispersed in Tris-Cl. Thus, the GO nanosheets have been reduced and the aromatic structure within the GO nanosheets restored upon dopamine reduction.[9,39] The structures of GO before and after reduction were also characterized by X-ray diffraction (XRD). As shown in Figure S1 (Supporting Information), the sharp diffraction peak in GO (*d*-spacing 8.29 Å at $2\theta = 10.7°$) has decreased dramatically after reduction, and a new broad diffraction peak (*d*-spacing 3.81 Å at $2\theta = 23.4°$) has appeared in the PDA-capped RGO.[9,40,41] This diffraction peak of PDA-capped RGO is closer to the typical diffraction peak of graphite (*d*-spacing 3.35 Å at $2\theta = 26.6°$),[18] indicating the successful reduction of GO. Furthermore, the sheet resistance of PDA-capped RGO ($\sim 10^8$ ohm/sq) is about 2 orders magnitude lower than that ($\sim 10^{10}$ ohm/sq) of GO, consistent with the reduction of latter.[9]

The X-ray photoelectron spectroscopy (XPS) C 1s core-level spectrum of GO nanosheets (Figure 3a) can be curved into five peak components with binding energies (BEs) at about 283.8, 284.6, 286.4, 287.9, and 288.8 eV, attributable to the sp^2-hybridized carbon, sp^3-hybridized carbon, *C*−O, *C*═O, and O−*C*═O species, respectively.[18,22,42,43] The XPS C 1s core-level spectrum of the PDA-capped RGO nanosheets (Figure 3b) can be curve-fitted into five peak components with BEs at about 284.6, 285.5, 286.4, 287.8, and 288.9 eV, attributable to the *C*−C, *C*−N, *C*−O, *C*═O, and O−*C*═O species, respectively.[42] The appearance of the C−N peak component at the BE of 285.5 eV in the C 1s core-level spectrum and an N 1s core-level spectrum at the BE of ~400 eV (inset of Figure 3b) is consistent with the presence of a surface-capped PDA layer. The C 1s core-level spectral line shape of PDA-capped RGO is similar to that of pure PDA obtained from self-polymerization of dopamine on a metal substrate (Figure S2, Supporting Information) and is consistent with the structure of PDA[44] having a theoretical C−C:C−N:C−O ratio of 4:2:2, suggesting that the RGO surface is dominated by the PDA adlayer. Figure S3 (Supporting Information) shows the thermogravimetric analysis (TGA) curves of the GO and PDA-capped RGO nanosheets at a heating rate of

*To whom correspondence should be addressed: E-mail: cheket@nus.edu.sg (E.-T.K.); fu7352@seu.edu.cn (G.D.F.).

 Published on Web 09/27/2010

Scheme 1. Schematic Illustration of the Preparation of PDA-Capped RGO and RGO-*g*-PEG[a]

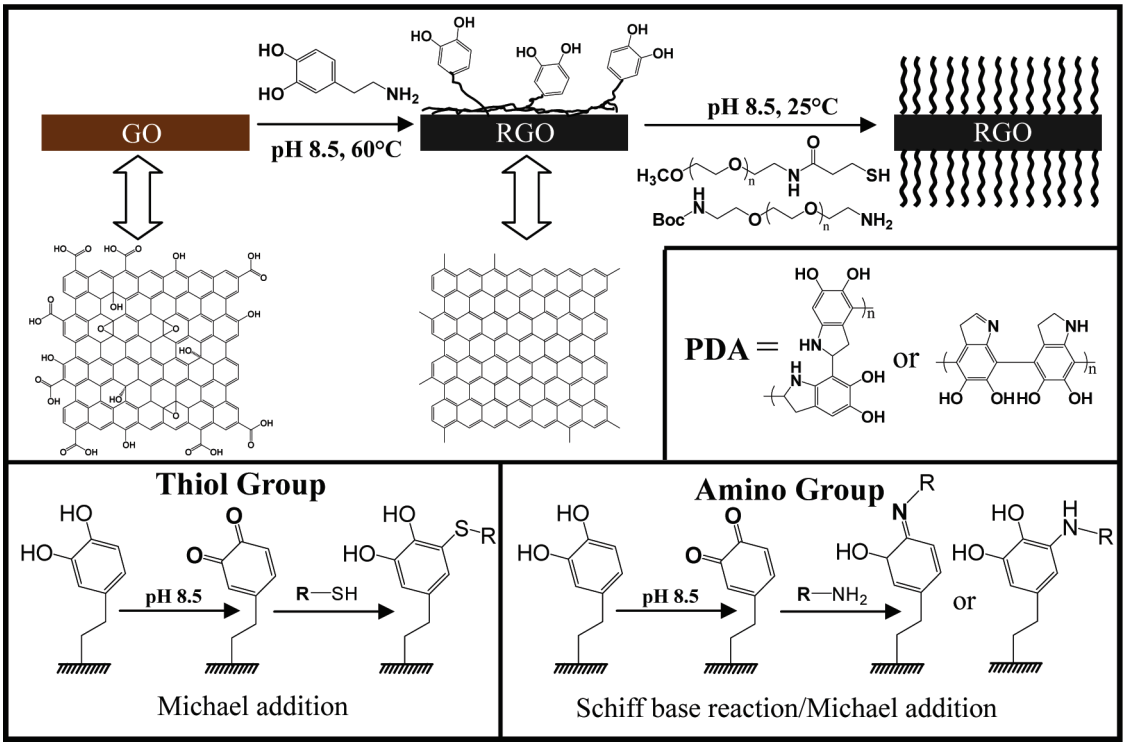

[a] GO = graphene oxide, PDA = polydopamine, RGO = reduced graphene oxide, and PEG = poly(ethylene glycol).

10 °C/min in air. GO is thermally unstable, with a rapid weight loss commences at about 200 °C. Dopamine reduction and PDA affinity appear to be effective in enhancing the thermal stability of GO nanosheets.

The PDA adlayer containing catechol groups is a versatile platform for further modification and functionalization of RGO with additional organic layers to enhance the dispersity of RGO in various solvents, such as water, tetrahydrofuran, dimethylformamide, and chloroform. At weak alkaline pH, the oxidized quinone form of catechol groups can react with thiol- and amino-terminated PEG via Michael addition and Michael addition/Schiff base reaction, respectively. The resulting PEG-grafted RGO (RGO-*g*-PEG) can be redispersed in various solvents and exhibits excellent stability in these dispersing media (Figure 1c). The maximum solubility of RGO-*g*-PEG in water can reach about 6.5 mg/mL. The successful grafting of PEG brushes on the surface of PDA-capped RGO was confirmed by XPS. Figure 3c shows the C 1s core-level spectrum of RGO-*g*-PEG nanosheets from grafting of the thiol-terminated PEG. It can be curve-fitted into five peak components with BEs at about 284.6, 285.4, 286.3, 287.8, and 288.9 eV, attributable to the *C*−C, *C*−N/*C*−S, *C*−O, *C*═O, and O−*C*═O species, respectively.[42] The marked increase in intensity of the *C*−O peak component and the appearance of the S 2p core-level signal (inset of Figure 3c) indicate that the thiol-terminated PEG brushes have been successfully grafted on the RGO surface. The C 1s core-level spectrum of the RGO-*g*-PEG surface from grafting of amino-terminated PEG (Figure 3d) can also be curved into five peak components with BEs at about 284.6, 285.4, 286.3, 287.8, and 288.9 eV, attributable to the *C*−C, *C*−N, *C*−O, *C*═O, and O−*C*═O species, respectively.[42] The dominance of the *C*−O peak component is again consistent with the presence of grafted PEG brushes. Figures S4a−c (Supporting Information) show the respective ^{1}H NMR spectra of PDA-capped RGO, RGO-*g*-PEG from thiol-terminated PEG, and RGO-*g*-PEG from amino-terminated PEG. After Michael addition or Schiff base reaction, a new chemical shift appears at 3.53 ppm, attributable to the methylene group of PEG, and is present in the RGO-*g*-PEG samples from both thiol- and amino-terminated PEG. Since the cross-linked DPA layer is insoluble in *d*-DMSO, the amount of PDA and grafted PEG cannot be quantitatively resolved from the NMR spectra.

The respective FT-IR spectra of GO, PDA-capped RGO, and RGO-*g*-PEG from thiol- and amino-terminated PEG are shown in Figure S5 (Supporting Information). The appearance of a strong absorption peak at 1100 cm^{-1}, characteristic of the C−O−C stretching, further confirms that PEG brushes have been grafted on the PDA-capped RGO nanosheets. The amount of grafted PEG brushes on the RGO-*g*-PEG nanosheets is about 50 wt %, as deduced from the extent of major weight loss at 280−350 °C, associated with the decomposition of PEG,[45] in the TGA curves for the RGO-*g*-PEG nanosheets prepared from thiol- and amino-terminated PEG (Figure S3, Supporting Information). The respective differential scanning calorimetry (DSC) scans of PDA-capped RGO, RGO-*g*-PEG from thiol-terminated PEG, and RGO-*g*-PEG from thiol-terminated PEG are shown in Figure S6 (Supporting Information). The DSC endotherm of RGO-*g*-PEG from amino-terminated PEG (M_w ∼ 2000) shows a crystalline melting peak at 79.4 °C, which is comparable to that (85.4 °C) of RGO-*g*-PEG from thiol-terminated PEG (M_w ∼ 5000). The melting temperatures are higher than that (∼60 °C) for the PEG homopolymer of comparable molecular weight.[46] Thus, the melting endotherm of the immobilized PEG segments has shifted toward a higher temperature.

In summary, it has been shown that graphene oxide (GO) nanosheets can be readily reduced by dopamine with simultaneous capping by polydopamine (from self-polymerization of dopamine) to provide a versatile platform for covalent grafting of functional polymer brushes. Not only does dopamine allow reduction of GO without the use of hazardous chemicals or

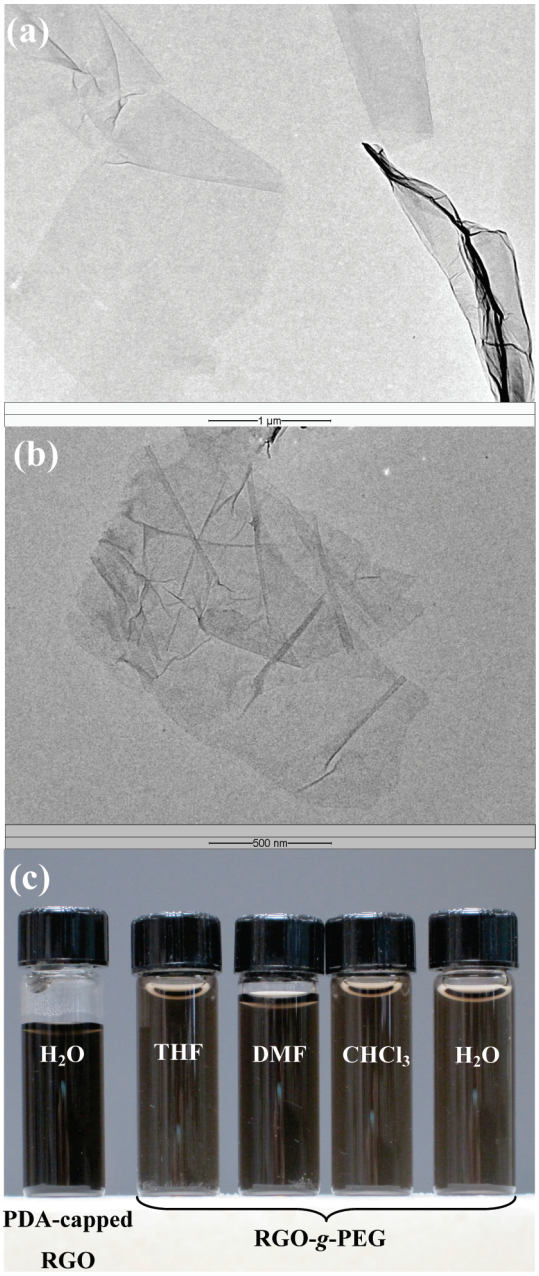

Figure 1. Transmission electron microscope (TEM) images of the (a) GO and (b) PDA-capped RGO nanosheets from aqueous dispersions. (c) Photograph of aqueous and organo-dispersions PDA-capped RGO and RGO-*g*-PEG after 1 week (concentrations of PDA-capped RGO in H_2O = 0.05 mg/mL and RGO-*g*-PEG in THF, DMF, $CHCl_3$, and H_2O = 0.02 mg/mL).

reducing agents, polydopamine can also be used to immobilize thiol- and amino-terminated PEG on the surface of reduced GO (RGO) in a "grafting-to" process. The PEG-grafted RGO nanosheets are organo- and water-dispersible (processable) and exhibit good stability in the dispersed state. The method will also allow the grafting of other thiol- or amino-functionalized molecules, polymers, and proteins, thus providing a versatile and benign means for the preparation and processing of graphene-based materials for biological and biomaterials applications.

Experimental Section. *Materials*. Natural graphite flakes, dopamine hydrochloride (98%), *O*-[2-(3-mercaptopropionylamino)ethyl]-*O*′-methylpoly(ethylene glycol) (thiol-terminated PEG, $M_w \sim 5000$), and *O*-(2-aminoethyl)-*O*′-[2-(boc-amino) ethyl]poly(ethylene glycol) (amino-terminated PEG, $M_w \sim 2000$) were purchased from Sigma-Aldrich Chem. Co. All other regents and solvents were purchased from either Sigma-Aldrich or Merck Chem. Co. and were used without further purification.

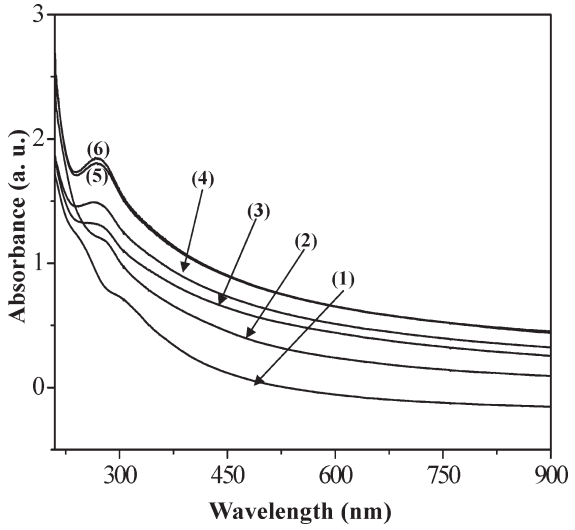

Figure 2. UV−vis spectra absorption of the Tris-Cl aqueous dispersions of GO (1) before and after being reduced by dopamine for (2) 4, (3) 8, (4) 12, (5) 16, and (6) 24 h.

Synthesis of Graphene Oxide (*GO*). GO was prepared via the modified Hummers method.[12] Typically, graphite (2 g, 500 mesh) and $NaNO_3$ (1 g) were mixed with concentrated H_2SO_4 (50 mL) in a 250 mL flask at 0 °C. The temperature was kept at 5 °C, and the mixture was stirred for 2 h. After that, 7.3 g of $KMnO_4$ was added in small portions to prevent temperature rise in excess of 20 °C. Then, the temperature of the reaction mixture was raised to 35 ± 2 °C, and the mixture was stirred for 30 min. After completion of the reaction, 90 mL of deionized water was gradually added into the solution. The suspension was reacted further by adding a mixture of H_2O_2 (7 mL, 30%) and water (55 mL). The graphene oxide was separated from the reaction mixture by filtration. The yellow-brown graphene oxide powders were washed three times with warm diluted HCl (3%, 150 mL) and then dried under reduced pressure for 24 h.

Synthesis of Polydopamine-Capped Reduced Graphene Oxide (*PDA-Capped RGO*). PDA-capped RGO was prepared typically as follows: 100 mg of GO and 50 mg of dopamine hydrochloride were added into 200 mL of 10 mM Tris-Cl solution (pH = 8.5) and dispersed by sonication for 10 min in an ice bath. The reaction mixture was stirred vigorously at 60 °C for 24 h, and changes in adsorption were monitored on a UV−vis photospectrometer. After the completion of the reduction reaction, the PDA-capped RGO was filtered with a 0.2 μm membrane filter, washed, redispersed, and dialyzed against distilled water for 3 days. The black powders were recovered by filtration and dried under reduced pressure for 24 h.

Synthesis of Poly(*ethylene glycol*) *Brush-Grafted RGO* (*RGO-g-PEG*). Surface modification of PDA-capped RGO was performed by adding 10 mg of the PDA-capped RGO and 20 mg of amino-terminated PEG (or 40 mg of thiol-terminated PEG) into 30 mL of 10 mM Tris-Cl solution (pH = 8.5). The reaction mixture was stirred at room temperature for 12 h. After that, the solution was filtered and washed thoroughly with deionized water and ethanol, followed by drying under reduced pressure for further characterization.

Characterization. Fourier transform infrared (FT-IR) spectroscopy measurements were carried out on a Bio-Rad

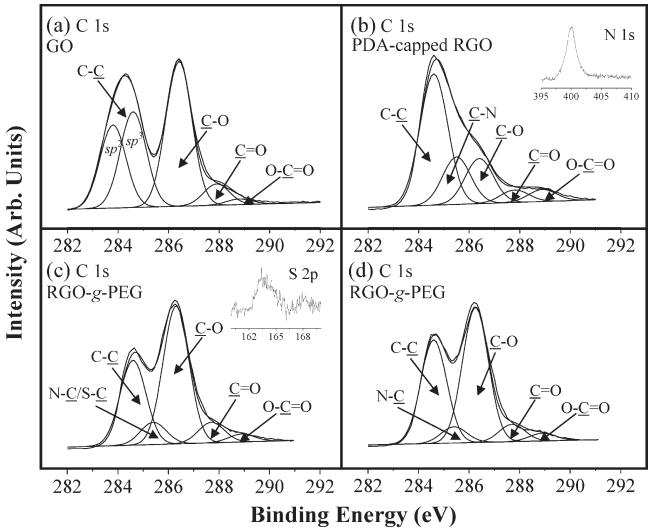

Figure 3. X-ray photoelectron spectroscopy (XPS) C 1s core-level spectra of (a) GO, (b) PDA-capped RGO, (c) RGO-*g*-PEG from thiol-terminated PEG, and (d) RGO-*g*-PEG from amino-terminated PEG. Insets of (b) and (c) are the N 1s and S 2p core-level spectra of PDA-capped RGO and RGO-*g*-PEG from thiol-terminated PEG, respectively. GO = graphene oxide, PDA = polydopamine, RGO = reduced graphene oxide, and PEG = poly(ethylene glycol).

FTS-135 spectrophotometer. X-ray photoelectron spectroscopy (XPS) measurements were carried out on a Kratos AXIS Ultra HSA spectrometer equipped with a monochromatized Al Kα X-ray source (1468.6 eV photons). Field emission transmission electron microscopy (FETEM) images were obtained from a JEOL JEM-2010 FETEM. The UV−vis absorption spectra in the wavelength range of 200−900 nm were obtained from a Shimadzu UV-3101PC spectrophotometer. Thermogravimetric analysis was carried out on a thermogravimetric analyzer (TGA, TA Instruments Model 2050) at a heating rate of 10 °C/min in air. Powder X-ray diffraction (XRD) measurements were carried out on a Shimadzu XRD-6000 apparatus, using the Cu Kα radiation. The DSC measurements were performed on a Pekin Elmer DSC7 calorimeter under a nitrogen atmosphere, at a heating rate of 10 °C/min. The ^{1}H NMR spectra were recorded on a Bruker ARX 300 MHz spectrometer, using *d*-DMSO as the solvent, in 1000 scans at a relaxation time of 2 s.

Supporting Information Available: XRD patterns of GO and PDA-capped RGO, XPS C 1s core-level spectrum of PDA, TGA traces of GO, PDA-capped RGO, and RGO-*g*-PEG, ^{1}H NMR spectra of PDA-capped RGO and RGO-*g*-PEG, FT-IR spectra of GO, PDA-capped RGO, and RGO-*g*-PEG, and DSC curves of PDA-capped RGO and RGO-*g*-PEG. This material is available free of charge via the Internet at http://pubs.acs.org.

References and Notes

(1) Novoselov, K. S.; Geim, A. K.; Morozov, S. V.; Jiang, D.; Katsnelson, M. I.; Grigorieva, I. V.; Dubonos, S. V.; Firsov, A. A. *Nature* **2005**, *438*, 197–200.
(2) Zhang, Y. B.; Tan, Y. W.; Stormer, H. L.; Kim, P. *Nature* **2005**, *438*, 201–204.
(3) Geim, A. K.; Novoselov, K. S. *Nature Mater.* **2007**, *6*, 183–191.
(4) Meyer, J. C.; Geim, A. K.; Katsnelson, M. I.; Novoselov, M. I.; Booth, T. J.; Roth, S. *Nature* **2007**, *446*, 60–63.
(5) Zhao, X.; Zhang, Q. H.; Chen, D. J.; Lu, P. *Macromolecules* **2010**, *43*, 2357–2363.
(6) Novoselov, K. S.; Geim, A. K.; Morozov, S. V.; Jiang, D.; Zhang, Y.; Dubonos, S. V.; Grigorieva, I. V.; Firsov, A. A. *Science* **2004**, *306*, 666–669.
(7) Dato, A.; Radmilovic, V.; Lee, Z. H.; Phillips, J.; Frenklach, M. *Nano Lett.* **2008**, *8*, 2012–2016.
(8) Stankovich, S.; Dikin, D. A.; Piner, R. D.; Kohlhaas, K. A.; Kleinhammes, A.; Jia, Y.; Wu, Y.; Nguyen, S. T.; Ruoff, R. S. *Carbon* **2007**, *45*, 1558–1565.
(9) Li, D.; Muller, M. B.; Gilje, S.; Kaner, R. B.; Wallace, G. G. *Nature Nanotechnol.* **2008**, *3*, 101–105.
(10) Park, S. J.; An, J. H.; Jung, I. H.; Piner, R. D.; An, S. J.; Li, X. S.; Velamakanni, A.; Ruoff, R. S. *Nano Lett.* **2009**, *9*, 1593–1597.
(11) Tung, V. C.; Allen, M. J.; Yang, Y.; Kaner, R. B. *Nature Nanotechnol.* **2009**, *4*, 25–29.
(12) Yang, H. F.; Shan, C. S.; Li, F. H.; Han, D. X.; Zhang, Q. X.; Niu, L. *Chem. Commun.* **2009**, *26*, 3880–3882.
(13) Shin, H. J.; Kim, K. K.; Benayad, A.; Yoon, S. M.; Park, H. K.; Jung, I. S.; Jin, M. H.; Jeong, H. K.; Kim, J. M.; Choi, J. Y.; Lee, Y. H. *Adv. Funct. Mater.* **2009**, *19*, 1987–1992.
(14) Wang, S.; Tambraparni, M.; Qiu, J.; Tipton, J.; Dean, D. *Macromolecules* **2009**, *42*, 5251–5255.
(15) Yamaguchi, H.; Eda, G.; Mattevi, C.; Kim, H.; Chhowalla, M. *ACS Nano* **2010**, *4*, 524–528.
(16) Zhu, Y. W.; Stoller, M. D.; Cai, W. W.; Velamakanni, A.; Piner, R. D.; Chen, D.; Ruoff, R. S. *ACS Nano* **2010**, *4*, 1227–1233.
(17) Lightcap, I. V.; Kosel, T. H.; Kamat, P. V. *Nano Lett.* **2010**, *10*, 577–583.
(18) Zhang, J. L.; Yang, H. J.; Shen, G. X.; Cheng, P.; Zhang, J. Y.; Guo, S. W. *Chem. Commun.* **2010**, *46*, 1112–1114.
(19) Gilje, S.; Dubin, S.; Badakhshan, A.; Farrar, J.; Danczyk, S. A.; Kaner, R. B. *Adv. Mater.* **2010**, *22*, 419–423.
(20) Zhu, C. Z.; Guo, S. J.; Fang, Y. X.; Dong, S. J. *ACS Nano* **2010**, *4*, 2429–2437.
(21) Xu, J. Z.; Chen, T.; Yang, C. L.; Li, Z. M.; Mao, Y. M.; Zeng, B. Q.; Hsiao, B. S. *Macromolecules* **2010**, *43*, 5000–5008.
(22) Liu, J. B.; Fu, S. H.; Yuan, B.; Li, Y. L.; Deng, Z. X. *J. Am. Chem. Soc.* **2010**, *132*, 7279–7281.
(23) Wang, G. X.; Shen, X. P.; Wang, B.; Yao, J.; Park, J. *Carbon* **2009**, *47*, 1359–1364.
(24) Cote, L. J.; Kim, F.; Huang, J. X. *J. Am. Chem. Soc.* **2009**, *131*, 1043–1049.
(25) Guo, S. J.; Dong, S. J.; Wang, E. K. *ACS Nano* **2010**, *4*, 547–555.
(26) Waite, J. H.; Tanzer, M. L. *Science* **1981**, *212*, 1038–1040.
(27) Lee, H.; Dellatore, S. M.; Miller, W. M.; Messersmith, P. B. *Science* **2007**, *318*, 426–430.
(28) Lee, H.; Lee, B. P.; Messersmith, P. B. *Nature* **2007**, *448*, 338–342.
(29) Lee, H.; Lee, Y.; Statz, A. R.; Rho, J.; Park, T. G.; Messersmith, P. B. *Adv. Mater.* **2008**, *20*, 1619–1623.
(30) LaVoie, M. J.; Ostaszewski, B. L.; Weihofen, A.; Schlossmacher, M. G.; Selkoe, D. J. *Nature Med.* **2005**, *11*, 1214–1221.
(31) Burzio, L. A.; Waite, J. H. *Biochemistry* **2000**, *39*, 11147–11153.
(32) Lee, Y.; Chung, H. J.; Yeo, S.; Ahn, C. H.; Lee, H.; Messersmith, P. B.; Park, T. G. *Soft Matter* **2010**, *6*, 977–983.
(33) Zhou, W. H.; Lu, C. H.; Guo, X. C.; Chen, F. R.; Yang, H. H.; Wang, X. R. *J. Mater. Chem.* **2010**, *20*, 880–883.
(34) Lee, H.; Lee, K. D.; Pyo, K. B.; Park, S. Y.; Lee, H. *Langmuir* **2010**, *26*, 3790–3793.
(35) Fei, B.; Qian, B. T.; Yang, Z. Y.; Wang, R. H.; Liu, W. C.; Mak, C. L.; Xin, J. H. *Carbon* **2008**, *46*, 1795–1797.
(36) Fu, Y. C.; Li, P. H.; Xie, Q. J.; Xu, X. H.; Lei, L. H.; Chen, C.; Zou, C.; Deng, W. F.; Yao, S. Z. *Adv. Funct. Mater.* **2009**, *19*, 1784–1791.
(37) Hummers, W. S.; Offerman, J. R. E. *J. Am. Chem. Soc.* **1958**, *80*, 1339–1339.
(38) Salavagione, H. J.; Gomez, M. A.; Matinez, G. *Macromolecules* **2009**, *42*, 6331–6334.
(39) Kong, B. S.; Geng, J. X.; Jung, H. T. *Chem. Commun.* **2009**, 2174–2176.
(40) Dikin, D. A.; Stankovich, S.; Zimney, E. J.; Piner, R. D.; Dommett, G. H. B.; Evmenenko, G.; Nguyen, S. T.; Ruoff, R. S. *Nature* **2007**, *448*, 457–460.
(41) Fang, M.; Wang, K. G.; Lu, H. B.; Yang, Y. L.; Nutt, S. *J. Mater. Chem.* **2010**, *20*, 1982–1992.
(42) Wagner, C. D.; Moulder, J. F.; Davis, J. E.; Riggs, W. M. In *Handbook of X-ray Photoelectron Spectroscopy*; Perkin-Elmer Corp.: Waltham, MA, 1992; pp 40, 45, 73.
(43) Diaz, J.; Paolicelli, G.; Ferrer, S.; Comin, F. *Phys. Rev. B* **1996**, *54*, 8064–8069.
(44) Cui, J. W.; Wang, Y. J.; Postma, A.; Hao, J. C.; Hosta-Rigau, L.; Caruso, F. *Adv. Funct. Mater.* **2010**, *20*, 1625–1631.
(45) Petersen, H.; Fechner, P. M.; Fischer, D.; Kissel, T. *Macromolecules* **2002**, *35*, 6867–6874.
(46) Gitsov, I.; Zhu, C. *Macromolecules* **2002**, *35*, 8418–8427.